

Supporting Information

2,4,6-Tri(hydroxy)-1,3,5-triphosphinine, $P_3C_3(OH)_3$: The Phosphorus Analogue of Cyanuric Acid

Riccardo Suter, Yanbo Mei, Matthew Baker, Zoltan Benkő,* Zhongshu Li, and Hansjörg Grützmacher**

anie_201610156_sm_miscellaneous_information.pdf

Supporting Information

Experimental:

General Considerations.

All air- and moisture-sensitive manipulations were carried out using standard vacuum line Schlenk techniques or in an MBraun inert atmosphere dry-box containing an atmosphere of purified argon. THF-*d*₈, CD₂Cl₂ and C₆D₆ were purchased from Cambridge Isotope Laboratories. CD₂Cl₂ was dried over CaH₂ and distilled, THF-*d*₈ and C₆D₆ were distilled over potassium. All glassware was stored in a 120°C oven for several hours and was degassed prior to use. Solvents were degassed prior to the filtration over alumina in the PureSolv-purification system by “inert”, the water content was determined by Karl Fischer titration. Solvents were additionally tested using a ketyl test to guarantee oxygen and moisture free conditions. DIP-Chloride was recrystallized from hexane prior to use. Na(OCP) (short for Na(OCP)(Dioxane)_{2.5})^[1], [Mo(Mes)(CO)₃]^[2] was synthesized following literature procedures.

¹H NMR spectra were recorded on Bruker spectrometers operating at 300, 400 and 500 MHz, ¹³C NMR at 75.46 MHz 100.61 MHz. ³¹P NMR at 101.28, 121.494 and 161.97 MHz, ²H NMR at 61.42 MHz and ⁹⁵Mo-spectra at 32.6 MHz. All ¹H and ¹³C NMR chemical shifts are reported relative to SiMe₄ using the ¹H (residual) and ¹³C chemical shifts of the solvent as a secondary standard. ⁹⁵Mo chemical shifts are reported relative to a 2M aqueous solution of Na₂MoO₄. Peak widths at half heights (in Hz) are given for broad signals. Infrared spectra were collected on a Bruker-alpha FT-IR-spectrometer. UV/Vis spectra were recorded on UV/VIS/NIR lambda-19-spectrometer in a cell with a 1 or 2 mm path length. Elemental analyses were performed at the Mikrolabor of ETH Zürich.

Single crystals suitable for X-ray diffraction were coated with polyisobutylene oil in a glovebox, transferred to a nylon loop and then transferred to the goniometer of a Bruker X8 APEX2 or D8-Venture diffractometer or on an Oxford Excalibur equipped with a molybdenum X-ray tube ($\lambda = 0.71073 \text{ \AA}$). Preliminary data was collected to determine the crystal system. The space group was identified and the data were processed using the Bruker SAINT+ program and corrected for absorption using SADABS. The structures were solved using direct methods (SHELXS) on OLEX2 completed by Fourier synthesis and refined by full-matrix least-squares procedures.

Preparation of compound $P_3C_3[OB(ipc)_2]_3$ (4): Na(OCP)(dioxane)_{2.5} (12.16 g, 40 mmol) was dissolved in 150 mL of THF and (ipc)₂B-Cl (12.8 g, 40 mmol) was dissolved in 100 mL of THF. The Na(OCP) solution was then added dropwise to the (ipc)₂B-Cl solution, which was cooled in an ice bath. The color changed from brown to red upon addition of the Na(OCP) solution. If the (-)-DIP-Cl is not pure a color change from brown to dark red was observed because excess Na(OCP) reacts with the ring. ¹¹B NMR spectroscopy indicated the total consumption of (ipc)₂B-Cl (δ = 74.6 ppm). The reaction mixture was dried under reduced pressure. The residue was dissolved in 100 mL of hexane, filtered through Celite and washed with hexane three times. The hexane solution was collected and dried under reduced pressure. The product was then dissolved in a 40 mL 1:1 mixture of THF and 1,4-dioxane. Under vigorous stirring, 150 mL MeCN was added drop wise to precipitate the product. The solid was filtered off, washed with MeCN and dried under reduced pressure to yield 12.2g (89%) of a pale white fluffy solid. Single crystals for X-ray diffraction analysis were grown from a dioxane ether solution upon slow evaporation of the solvent. MF: C₆₃H₁₀₂B₃O₃P₃, MW: 1032.73 g/mol, MP: 196 °C, EA[calc]: C, 73.26; H, 9.95; EA[found]: C, 71.58; H, 10.02. Absorption max [λ nm]: 302, 329 shoulder, CCDC 1454807, ³¹P-NMR (C₆D₆, 121.5 MHz): δ (ppm) = 183.4 (s, 3P); ¹H-NMR (C₆D₆, 300 MHz): δ (ppm) = 2.62 (m, 1H, CH), 2.38 (m, 1H, CH), 2.15 – 1.9 (m, 4H, CH), 1.85 (m, 1H, CH), 1.18 (s, 3H, CH₃), 1.13 (d, J = 7.1 Hz, 3H, CH₃), 1.05 (s, 3H, CH₃); ¹³C{¹H}-NMR (C₆D₆, 75 MHz): δ (ppm) = 226.6 (m, 3C, aromatic C), 48.03 (s), 41.28 (s), 38.8 (s), 37.6 (s), 33.7 (s), 29.3 (s), 28.3 (s), 27.0 (s), 23.3 (s), 22.8 (s); IR [cm⁻¹] powder: 2942.59, 2895.67, 2866.75, 1449.79, 1365.10, 1305.30, 1257.20, 1223.85, 1173.02, 1134.60, 1083.22, 1047.46. No signal was observed in the ¹¹B-NMR spectrum even with a large number of scans. ¹¹B is a quadrupolar ($I=3/2$) nucleus and thus when in environments with lower than tetrahedral symmetry the electric field gradient across the nucleus can lead to very rapid relaxation and in turn lines several kHz broad making observation very difficult.

Preparation of compound [Mo{P₃C₃[OB(ipc)₂]₃}(CO)₃] (7): P₃C₃[OB(ipc)₂]₃ **4** (100 mg, 0.1 mmol) was dissolved in 4 mL of hexane and was added dropwise to a solution of [Mo(Mes)(CO)₃] (30 mg, 0.1 mmol) in 4 mL of dioxane. The reaction mixture turned dark red to brown and was left unstirred for 12 hours. The volatiles were removed under reduced pressure and the brown solid was dissolved in 4 mL of methyl(*tert*-buthyl)ether MTBE and was filtered through a glass filter paper. Under slow evaporation of the solvent yellow needles covered with red oil were isolated. The crystals were washed with a minimum (0.5 mL) of cold hexane. The washing solution was diluted with 2 mL of MTBE and the same procedure was repeated to isolate 42 mg of an analytical pure material (34 %). The washing solution still showed a high concentration of product. Repeating the procedure increased the yield significantly to totally 84 mg (69 %). Single crystals for X-ray diffraction analysis were grown from a saturated MTBE solution by slow evaporation of the solvent. MF: C₆₆H₁₀₂B₃O₆P₃Mo, MW: 1212.80 g/mol, MP: 196 °C, EA[calc]: C, 65.36; H, 8.48; EA[found]: C, 65.49; H, 8.58. Absorption max [λ nm]: 331.5 306.0, CCDC 1454806, ³¹P{¹H}-NMR (C₆D₆, 121.5 MHz): δ (ppm) = 7.4 (s, 3P); ¹H-NMR (C₆D₆, 300 MHz): δ (ppm) = 2.57 (m, 1H, CH), 2.41 (m, 1H, CH), 2.2 – 2.04 (m, 2H, CH), 2.00 (m, 1H, CH), 1.22 (s, 3H, CH₃), 1.98 (s, 1H, CH), 1.14 (pseudo-d, J = 7.0 Hz, 6H, CH₃); ¹³C{¹H}-NMR (C₆D₆, 100.6 MHz): δ (ppm) = 219.3 (s, CO), 156.94 (m, C_{arom}), 48.0 (s), 41.3 (s), 38.8 (s), 37.6 (s), 34.0 (s), 29.6 (s), 28.4 (s), 27.0 (s), 23.5 (s), 22.9 (s); ⁹⁵Mo-NMR (C₆D₆, 32.6 MHz): δ (ppm) = -1570 ppm; IR [cm⁻¹] solid: 2894.62, 2022.44 (s, CO), 1971.56 (s, CO), 1450.10, 1364.64, 1304.70, 1260.30, 1222.45, 1177.45, 1128.69, 1081.27, 1031.00

Preparation of compound [Mo{P₃C₃[OSi*t*Bu(Ph)₂]₃}(CO)₃] (8): A solution of P₃C₃[OB(ipp)₂]₃ **4** (205.7 mg, 0.2 mmol) in 5 mL THF was added dropwise to a stirred solution of *t*BuOH (574 μ L, 6 mmol) in 15 mL THF at 23 °C. The C₃P₃(OH)₃ formed immediately. *t*BuPh₂SiCl (468 μ L, 1.8 mmol) was added as a solid and a 5 mL THF solution of DBU (89 μ L, 0.6 mmol) was added dropwise at 23 °C to the reaction mixture. Then [MesMo(CO)₃] (90 mg, 0.3 mmol) was added as a solid to the reaction mixture. The red solution became dark red and a precipitate was formed. After stirring for another 0.5 h, the volatiles were removed under reduced pressure. The residue was extracted with hexane, filtered through Celite and washed several times with hexane. The filtrate was collected and reduced to 2 mL. Then 2 mL of dry acetonitrile was added to the clear solution. Slow evaporation of the solvent yielded yellow needles. The mixture was filtered and was washed with dry pentane three times to yield [Mo{P₃C₃[OSi*t*Bu(Ph)₂]₃}(CO)₃] (**8**) (32 mg, 15%). Yellow crystals suitable for X-ray analysis were obtained from a 1/1 mixture of MTBE/hexane. MF: C₅₄H₅₇O₆P₃Si₃Mo, MW: 1075.18, MP: 198 °C, EA[calc]: C, 60.33; H, 5.34; EA[found]: C, 58.23; H, 5.49. Absorption max [λ nm]: 319.5, 292.0, CCDC 1454805; ³¹P{¹H}-NMR (d₈-THF, 161.9 MHz): δ (ppm) = 16.1 (s, 3P); ¹H-NMR (d₈-THF, 400 MHz): δ (ppm) = 7.49-7.46 (m, 4H, Ph), 7.40-7.36 (m, 2H, Ph), 7.30-7.24 (m, 4H, Ph), 1.03 (s, 9H, CH₃); ¹³C{¹H}-NMR (d₈-THF, 100.6 MHz): δ (ppm) = 223.5 (s, CO), 163.9 (m, C_{arom}), 137.3 (s, Ph), 131.9 (s, Ph), 131.0 (s, Ph), 128.3 (s, Ph), 27.2 (s, *t*-Bu), 20.2 (s, *t*-Bu); ⁹⁵Mo-NMR (d₈-THF, 32.6 MHz): δ (ppm) = -1580 ppm; IR powder (cm⁻¹): 3069.69, 2930.28, 2857.48, 1992.79 (s, CO), 1941.42 (sh, CO), 1928.86 (s, CO), 1470.26, 1463.90, 1427.28, 1113.52, 1103.19, 1078.14, 1062.20, 1030.30, 1005.24, 997.84, 821.78, 790.56, 755.63, 733.93, 710.46, 694.48, 611.88, 586.96, 534.87, 511.30, 499.24, 484.57, 479.45, 452.75, 417.11

In situ formation of compound P₃C₃(OH)₃ (5): Compound **4** (110 mg, 0.1 mmol) was dissolved in 0.5 mL of d₈-THF. Subsequently 135 μ L of *t*BuOH (1.4 mmol) were added and the reaction mixture was directly analyzed by NMR.

³¹P{¹H}-NMR (d₈-THF, 161.9 MHz): δ (ppm) = 133.73 (s, 3P); ¹H-NMR (d₈-THF, 400 MHz): δ (ppm) = 11.18 (broad, 3H, O-H); ¹³C{¹H}-NMR (d₈-THF, 100.6 MHz): δ (ppm) = 231.3 (m, PC),

IR solution in THF [cm⁻¹]: 3154 (broad but small intensity, assigned to the OH frequency)

EI⁺-MS of a CH₂Cl₂ did not show the C₃H₄O₃P₃⁺ ion (180.94 m/z) the major fragment was assigned to the camphor groups (137.13 m/z).

In situ formation of compound P₃C₃(OD)₃ (5-d₃): Compound **4** (110 mg, 0.1 mmol) was dissolved in 0.5 mL of THF, MeOD (50 μ L, 1.25 mmol) was added and the mixture was directly analyzed by NMR.

³¹P{¹H}-NMR (THF, 161.9 MHz): δ (ppm) = 133.4 (s, 3P); ²H-NMR (THF, 400 MHz): δ (ppm) = 10.00 (3D, O-D);

Decomposition of compound P₃C₃(OH)₃ (5): **4** (71 mg, 0.07 mmol) was dissolved in 0.5 mL of C₆D₆ to this solution 0.05 mL of dry methanol was added. The reaction mixture was analysed directly after the addition by means of heteronuclear NMR spectroscopy. ³¹P{¹H}-NMR (d₈-THF, 161.9 MHz): δ (ppm) = 135.28 (s, 3P); The product decomposed overnight to form different phosphorus containing products. The reaction mixture was analysed by ³¹P-NMR spectroscopy, revealing the formation of PH₃ (δ (ppm) = -242.6 (q, ¹J_{P,H} = 186.9 Hz) and a RPH₂ compound at δ (ppm) = -138.3 (t, ¹J_{P,H} = 216.7 Hz) and a R₂PH species at δ (ppm) = -63.3 (d, ¹J_{P,H} = 242.4 Hz)

In situ formation of compound [Mo{P₃C₃(OH)₃}(CO)₃] (9): A 6 mL THF solution of P₃C₃[OB(ipc)₂]₃ (**4**) (256 mg, 0.25 mmol) and [Mo(Mes)(CO)₃] (92 mg, 0.25 mmol) was stirred at 23 °C for 1h. The red mixture was dried, dissolved in 5 mL hexane and filtrated. The filtrate containing **7** was collected and dried to give brown solid. 20 mg of **7** were dissolved in 0.5 mL d₈-THF in a NMR tube and 0.15 mL of degassed H₂O was added. After vigorous shaking, NMR spectra were taken. ³¹P{¹H}-NMR (d₈-THF, 161.9 MHz): δ (ppm) = -4.88 (s, 3P); ¹³C{¹H}-NMR (d₈-THF, 100.6 MHz): δ (ppm) = 224.6 (s, CO), 170.5 (m, PC ring). The ¹H-NMR (d₈-THF, 400 MHz) shows no resonance for the OH groups attached to the ring indicating rapid exchange on the NMR time scale. IR THF/H₂O solution (cm⁻¹): 1988.37 (s, CO), 1924.68 (s, CO).

Table S1: Compared spectroscopic and structural data of the isolated compounds. Angles are given in °, bond distances in Å, ³¹P-NMR, ¹³C-NMR chemical shifts in ppm. Data are from reference a^[3] b^[4] c^[5]

Compound	P-C-P (°)	C-P-C (°)	C-P (Å)	³¹ P (δ ppm)	¹³ C (δ ppm)	⁹⁵ Mo (δ ppm)
4	136.0	104.0	1.736	183.4	226.6	-
5	-	-	-	133.7	231.3	-
6	-	-	-	177.5	-	-
7	138.7	101.2	1.765	7.4	156.9	-1570
8	137.9	101.9	1.768	16.1	163.9	-1578
^t Bu ₃ C ₃ P ₃	130.7 ^a	109.3 ^a	1.727 ^a	232.6 ^b	211.8 ^b	-
^t Bu ₃ C ₃ P ₃ - Mo(CO) ₃	131.8 ^c	108.2 ^c	1.753 ^c	57.6 ^c	215.3 ^c	-

SPECTRA:

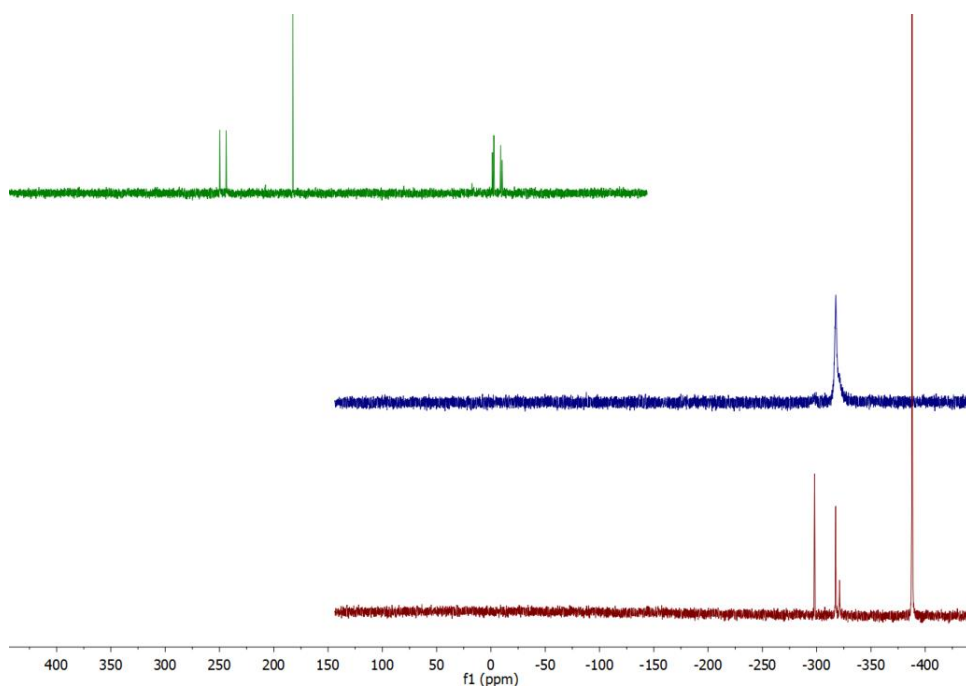


Figure S1: The Na(OCP) **1** solution in THF was cooled down to -78°C and was layered with a solution of the $(\text{ipc})_2\text{B-Cl}$ **2** in THF. The NMR tube was placed in a pre-cooled spectrometer without mixing the two liquids beforehand. From bottom to top. A) reaction mixture at 233 K, after layering the Na(OCP) solution with the $(\text{ipc})_2\text{B-Cl}$. -321.15 ppm (s, 1P) $\text{R}_2\text{B-P=C=O}$, -317.4 (s, 1P) $\text{R}_2\text{B-P=C=O}^*$, -297.97 (s, 1P) $\text{R}_2\text{B-O-C}\equiv\text{P}$. B) After mixing the reaction and warming up to 250 K. Only the $\text{R}_2\text{B-P=C=O}$ species are left, as a broad peak at -320.2 ppm. C) Reaction warmed up to 280 K. The product (182.7 ppm) and several unknown products were formed.

Figure S2: A triple resonance broad-band (TBI) probe, with $^1\text{H}/^2\text{D}/^{31}\text{P}/\text{BB}$ channels, was used to measure a ^{13}C ^{31}P HMQC of compound **4**.

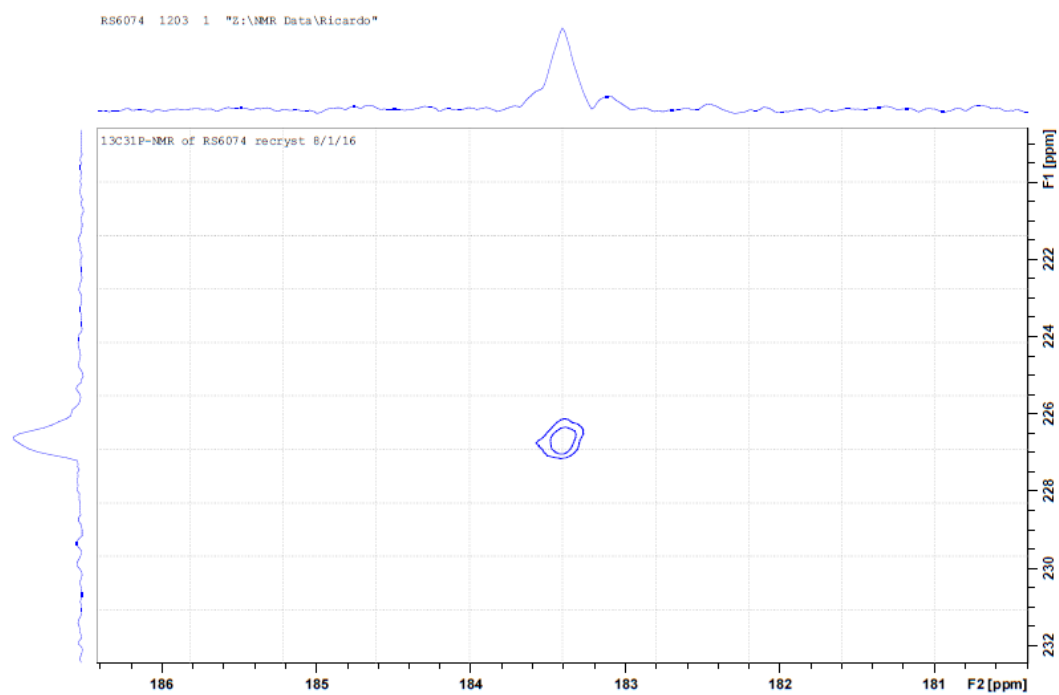


Figure S3: ^{31}P -NMR-spectra of Compound **4**

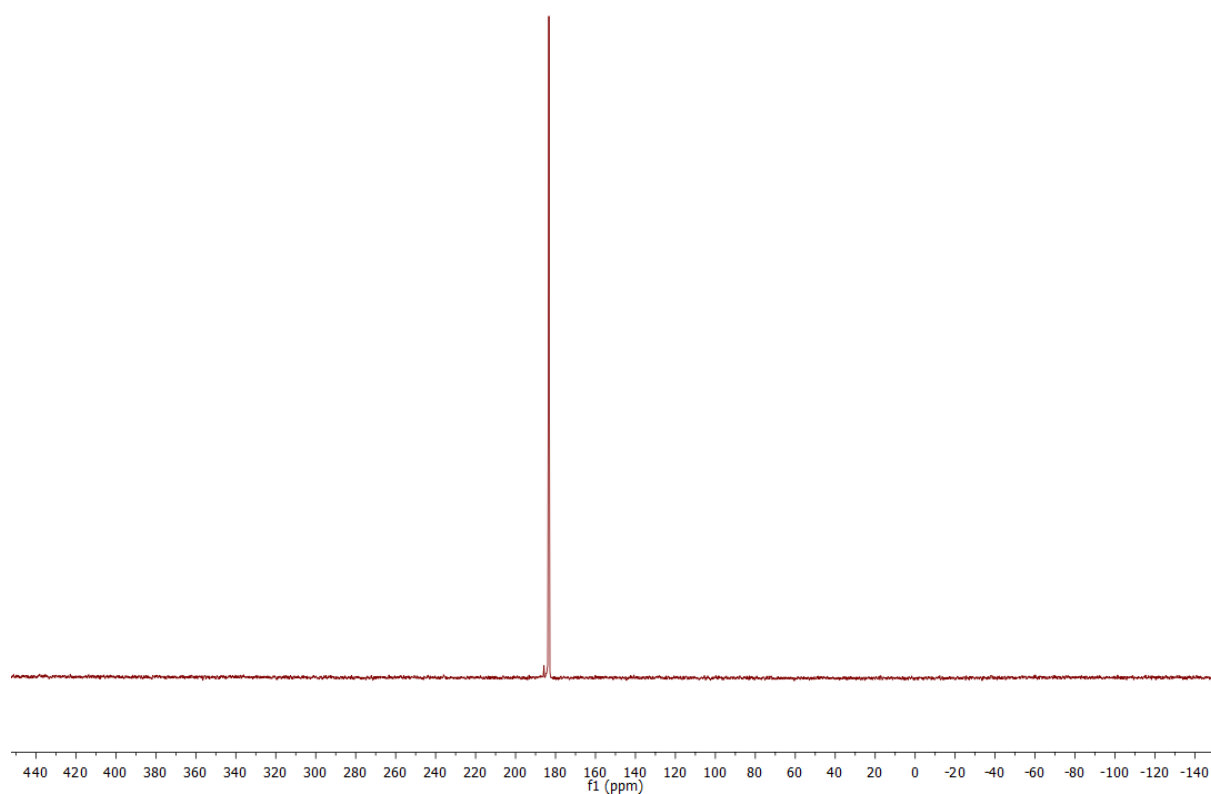


Figure S4: ^1H -NMR-spectra of Compound **4**

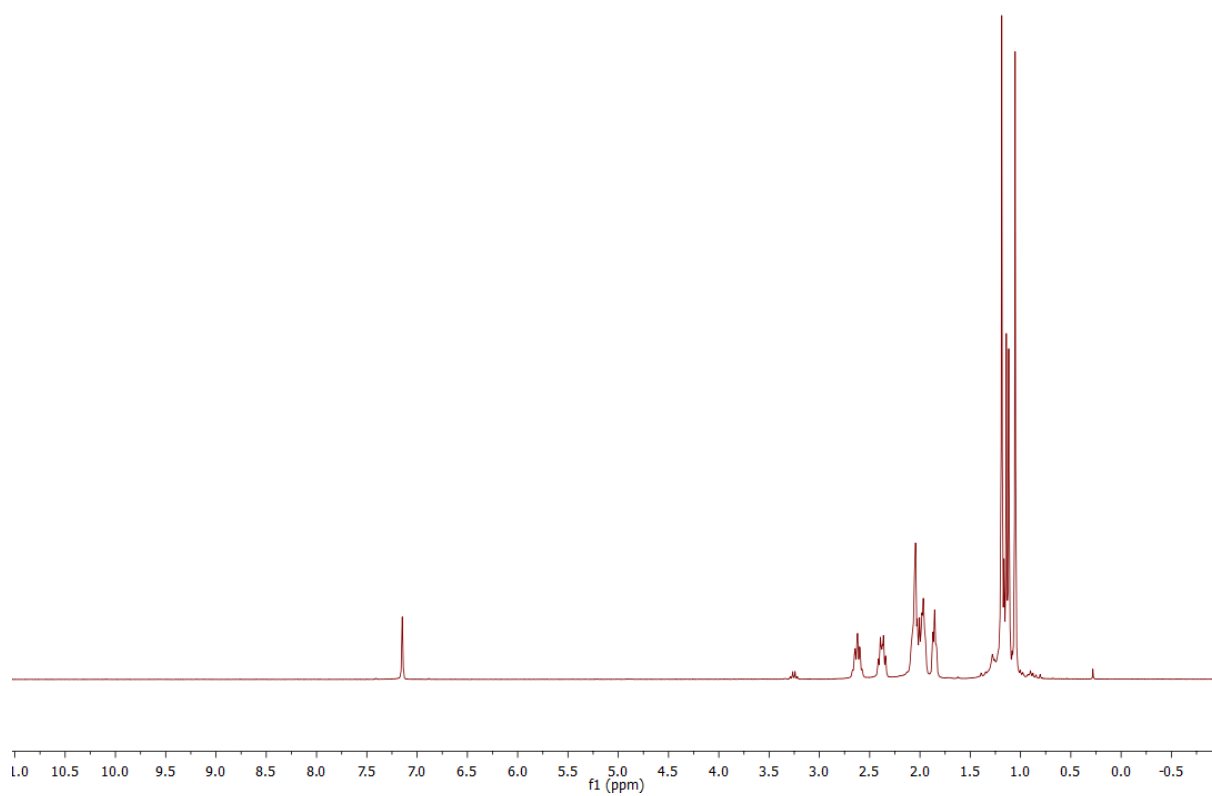


Figure S5: ^1H -NMR spectrum in THF- d_8 of compound **5**

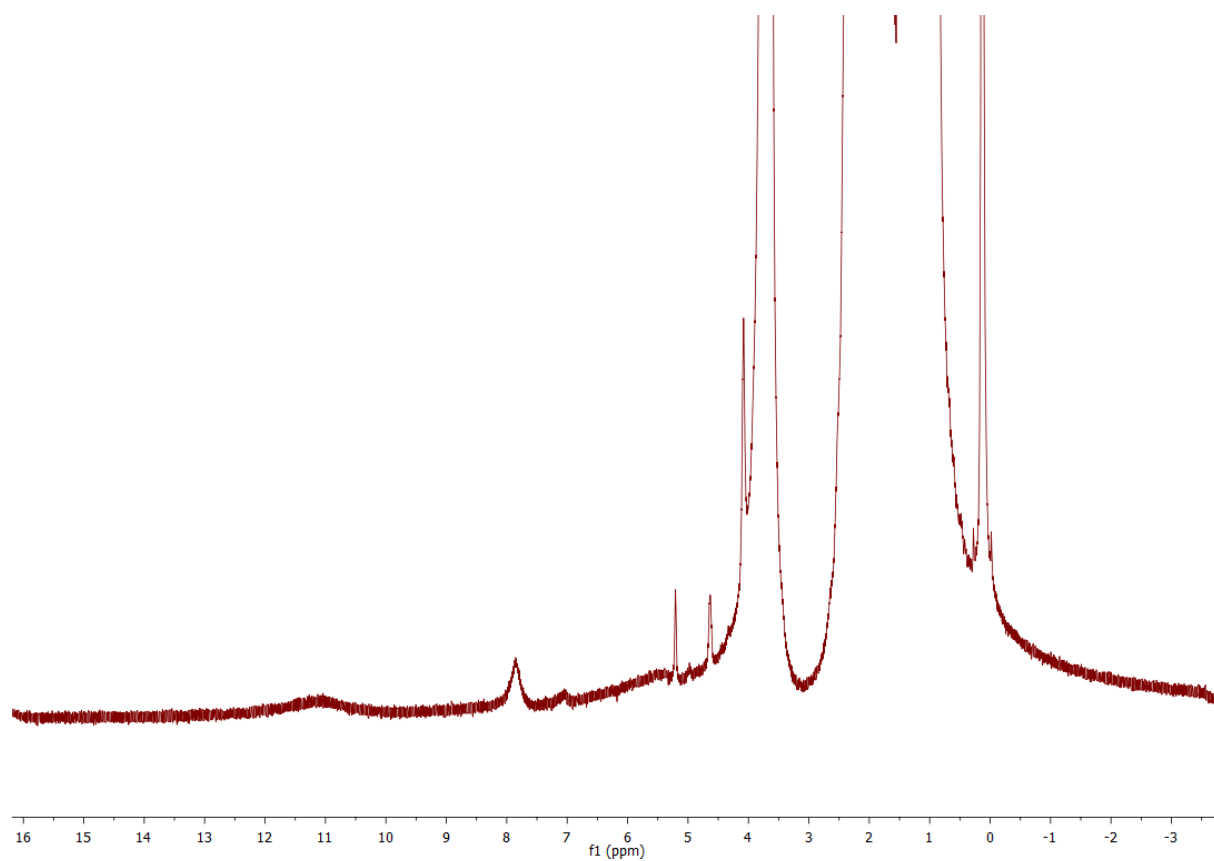


Figure S6: Detail view of the carbon ring atom in the ^{13}C -NMR spectrum in THF- d_8 for compound **5**

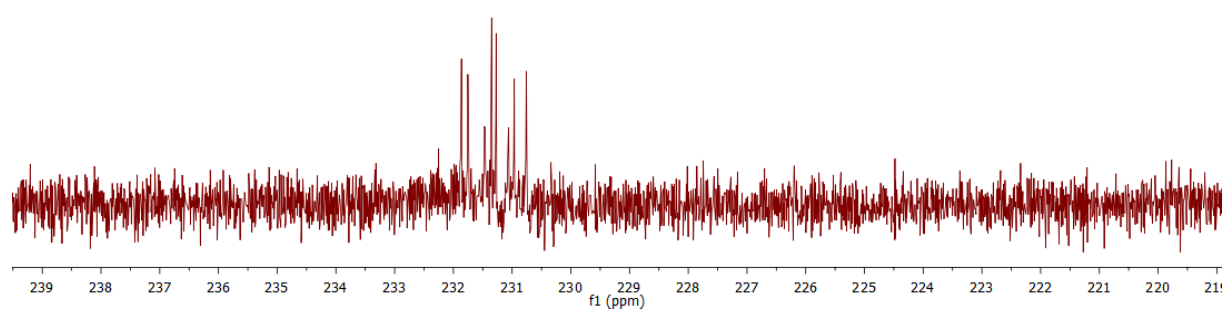


Figure S7: ^{31}P -NMR spectrum in THF- d_8 of compound **5**

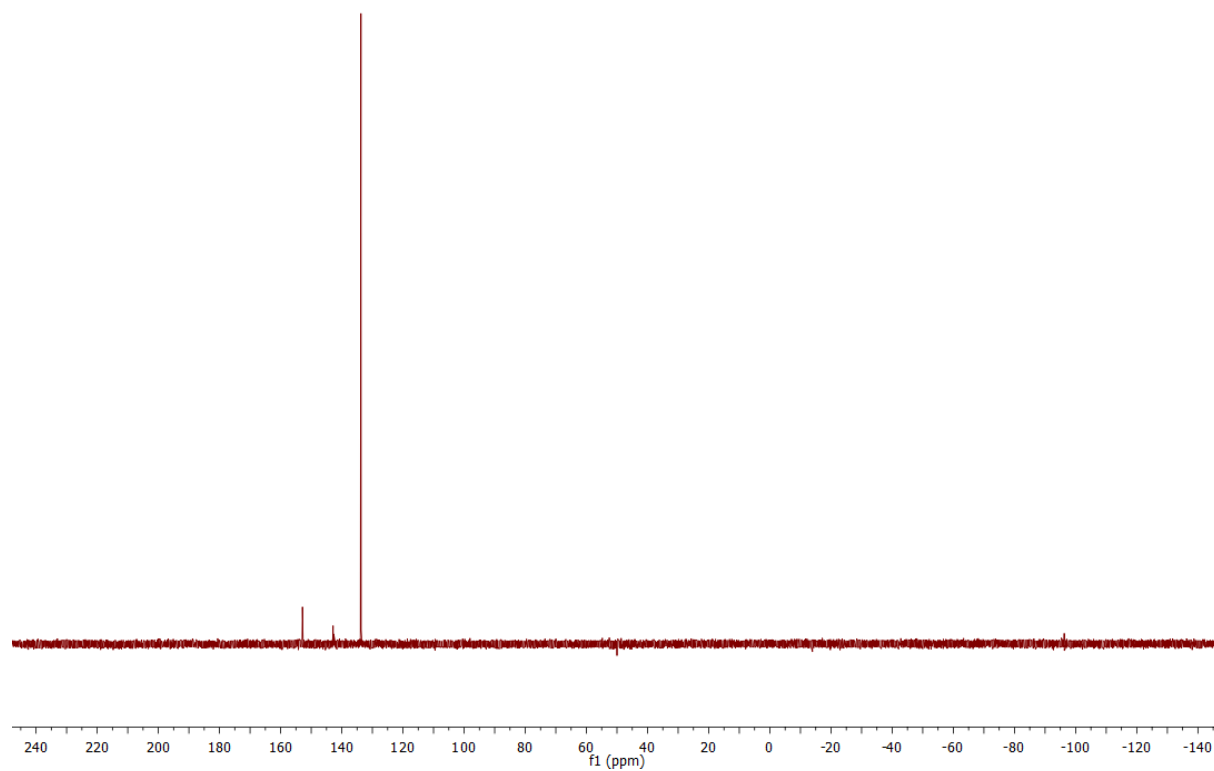


Figure S8: ^2H -NMR spectrum of compound **5-d3** in THF

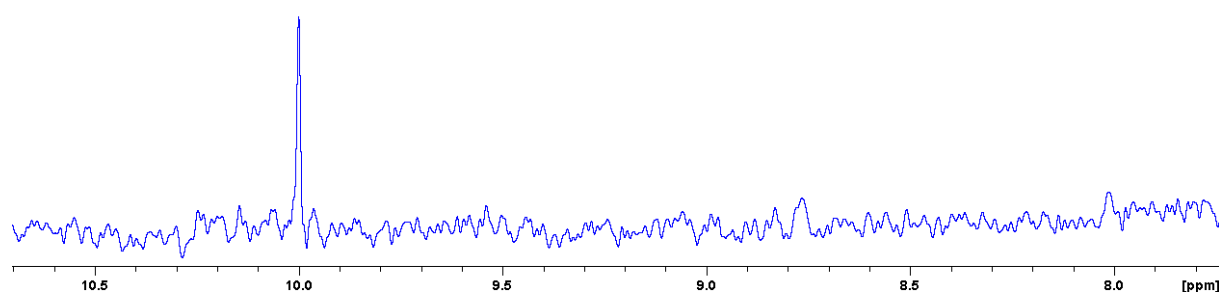


Figure S9: A triple resonance broad-band (TBI) probe, with $^1\text{H}/^2\text{D}/^{31}\text{P}/\text{BB}$ channels, was used to measure a ^{13}C ^{31}P HMQC of compound **7**

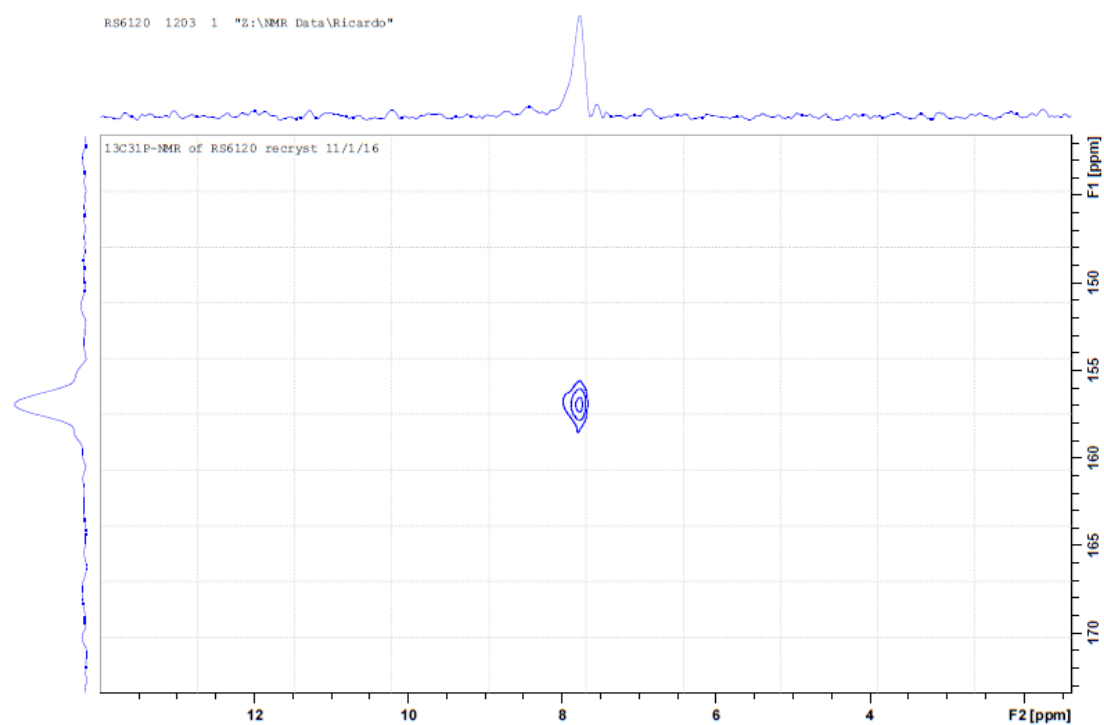


Figure S10: ^{95}Mo -NMR-spectra of Compound **7**

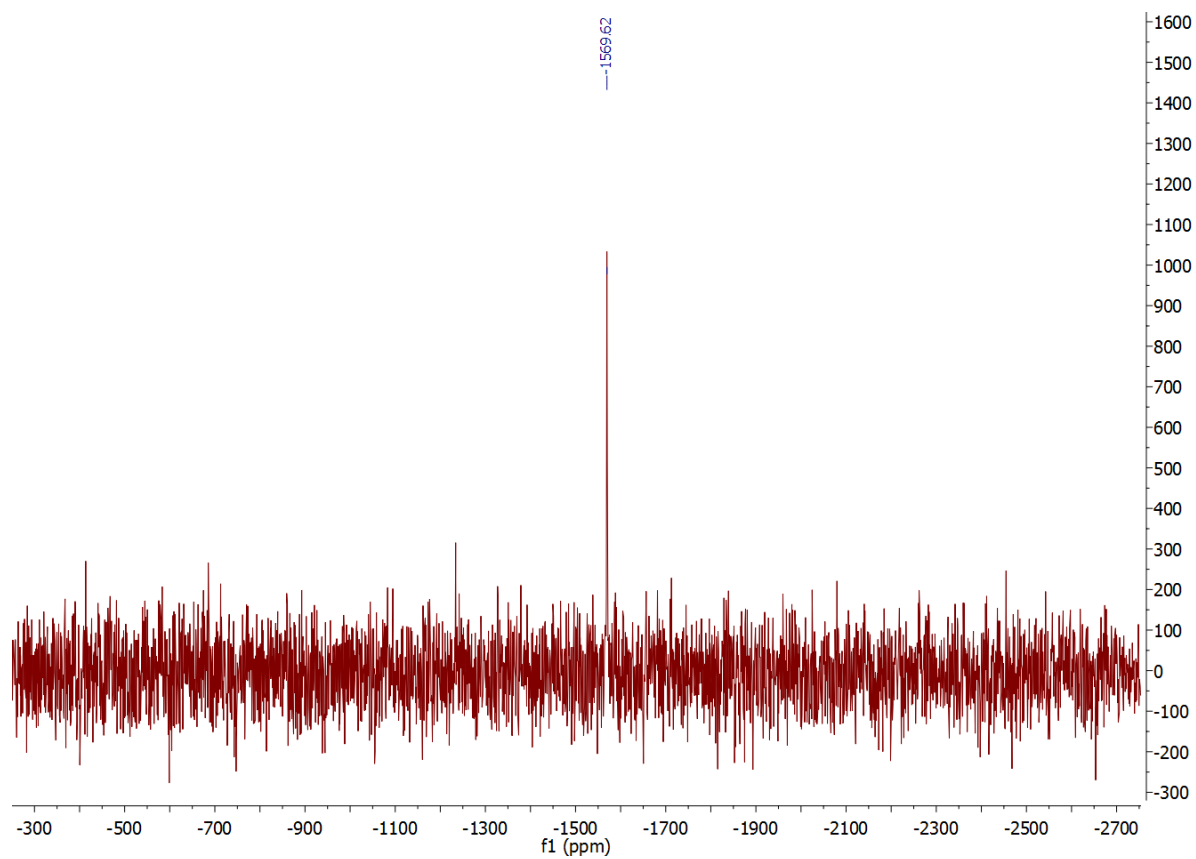


Figure S11: ^{31}P -NMR-spectra of Compound **7**

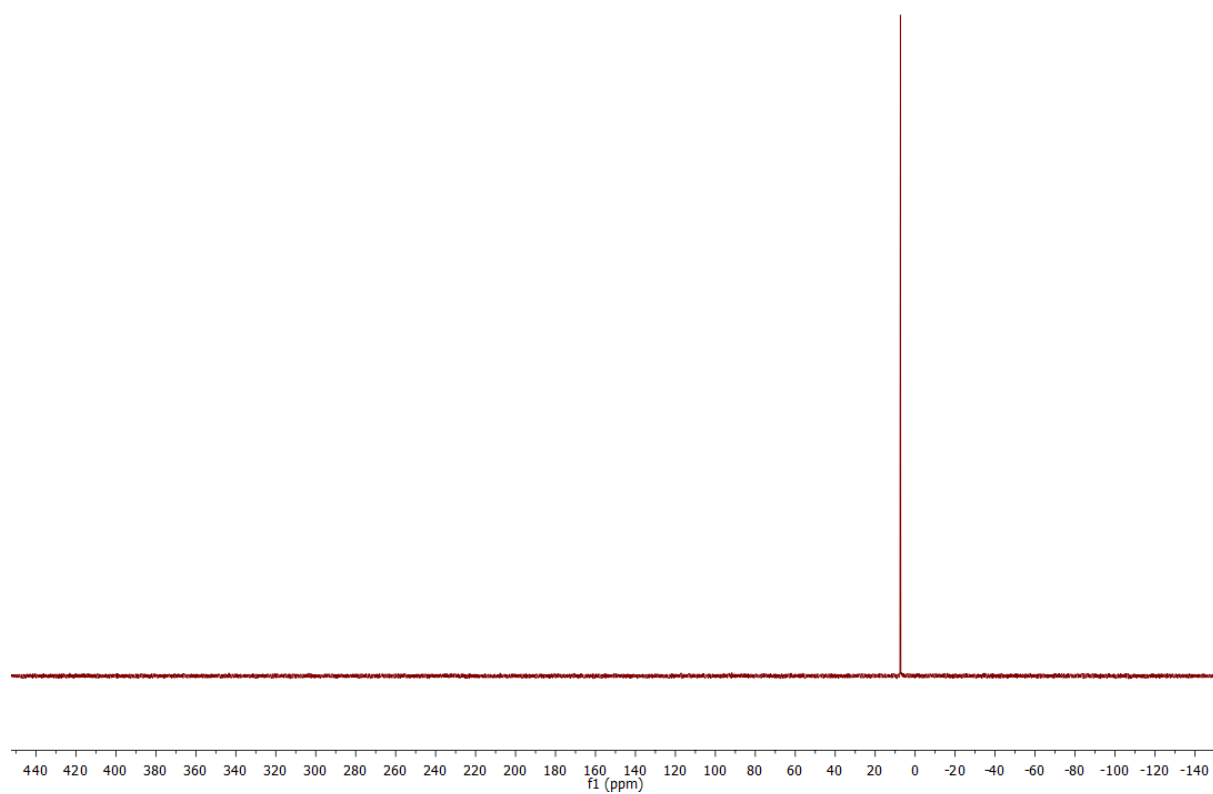


Figure S12: ^{13}C -NMR-spectra of Compound **7**

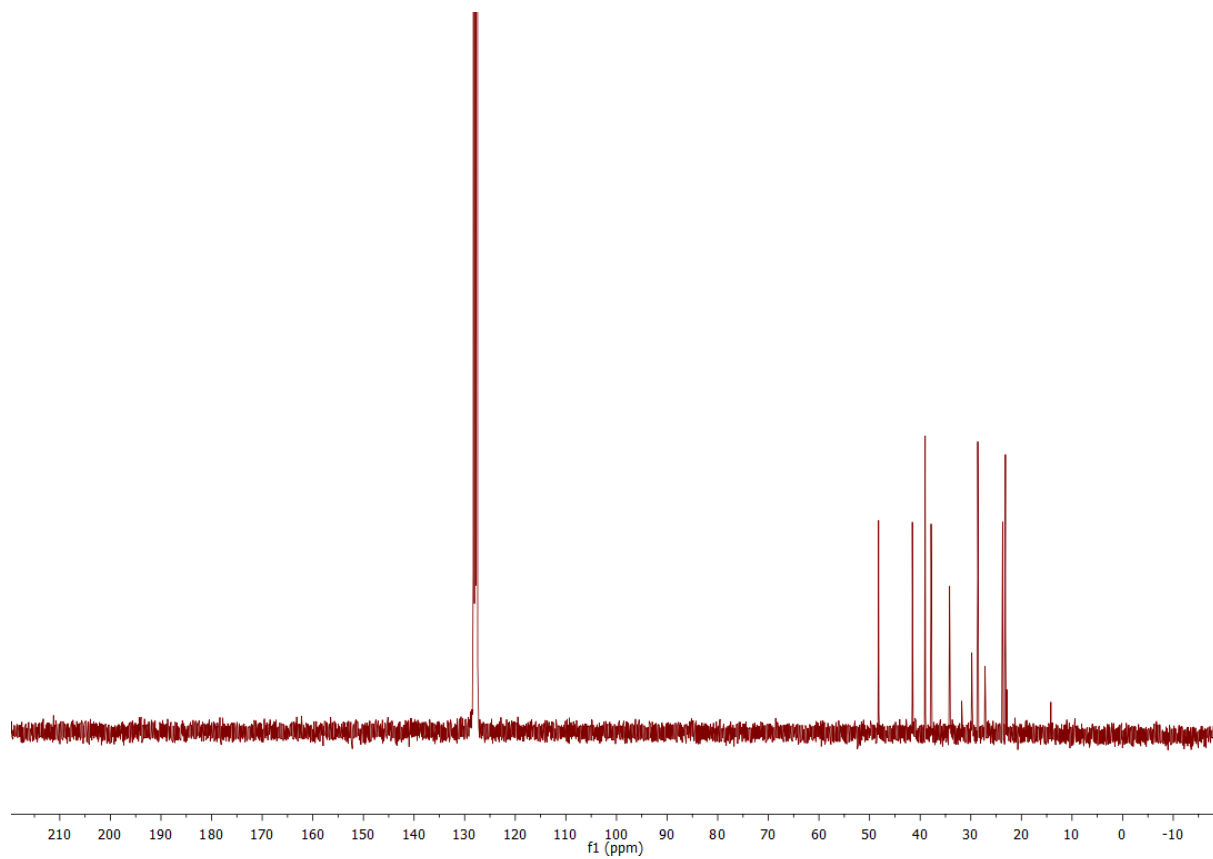


Figure S13: ^1H -NMR-spectra of Compound **7**

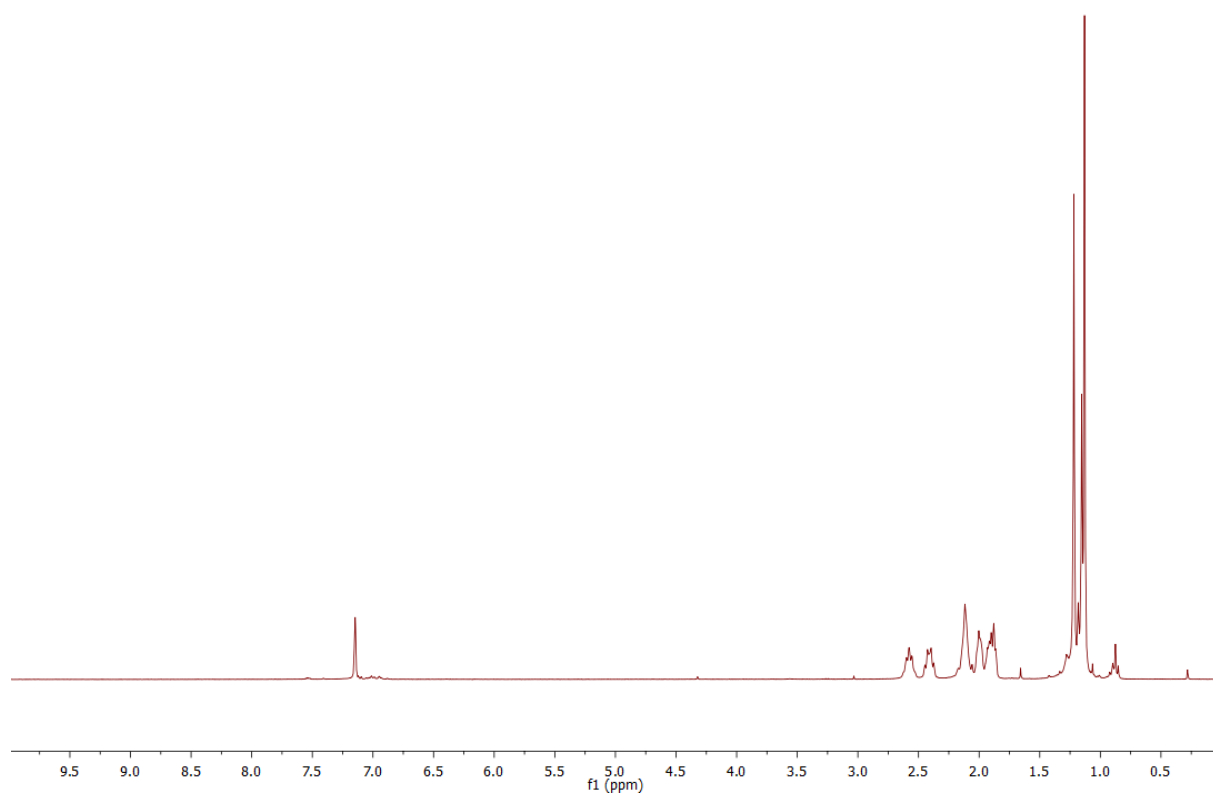


Figure S14: Solid state ATR-IR spectrum of compound **7**

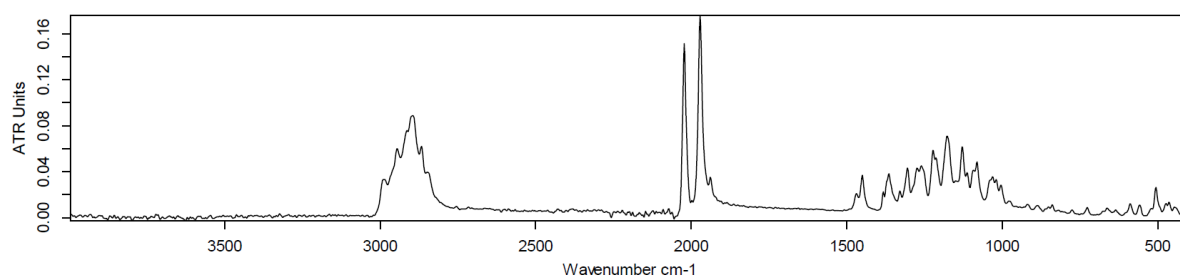


Figure S15: ^{95}Mo -spectra of Compound **8**

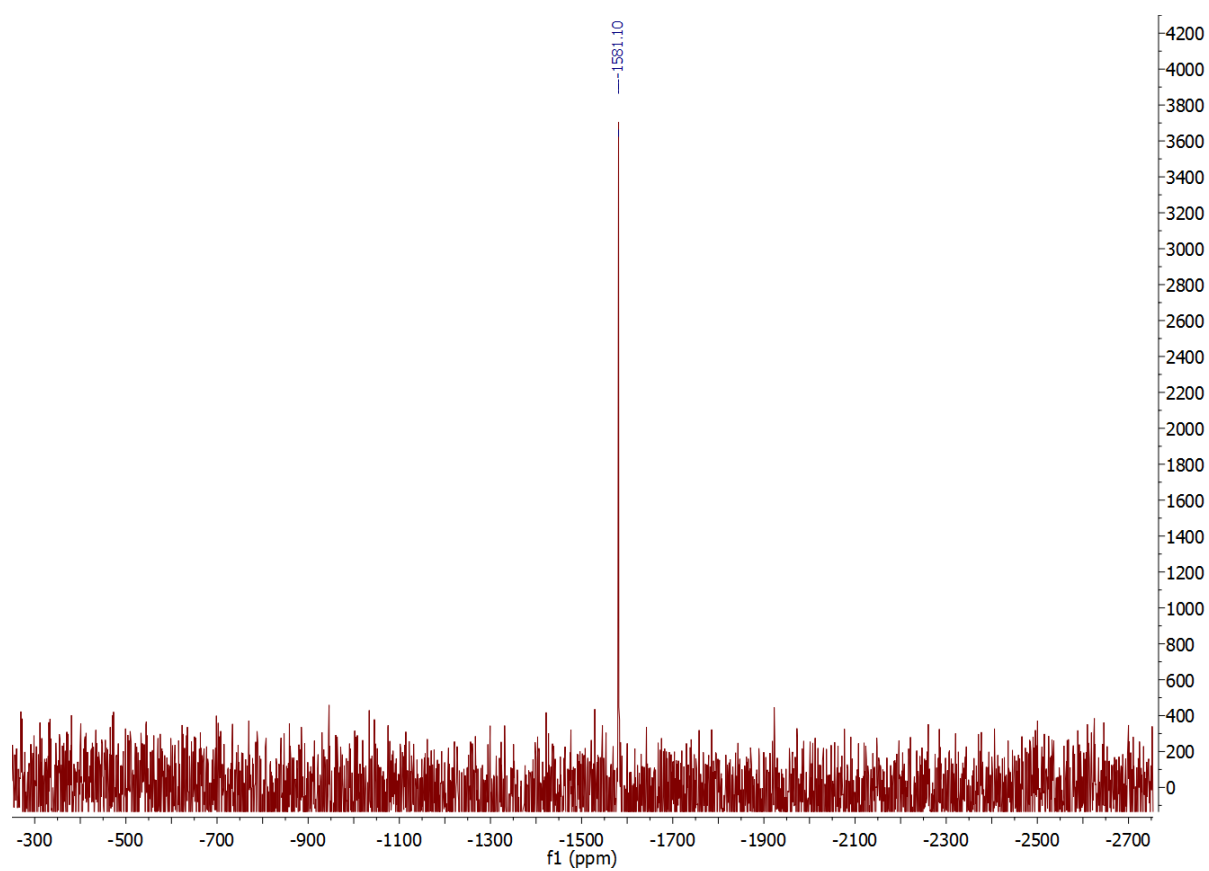


Figure S16: ^{13}C -NMR Spectrum of compound **8**

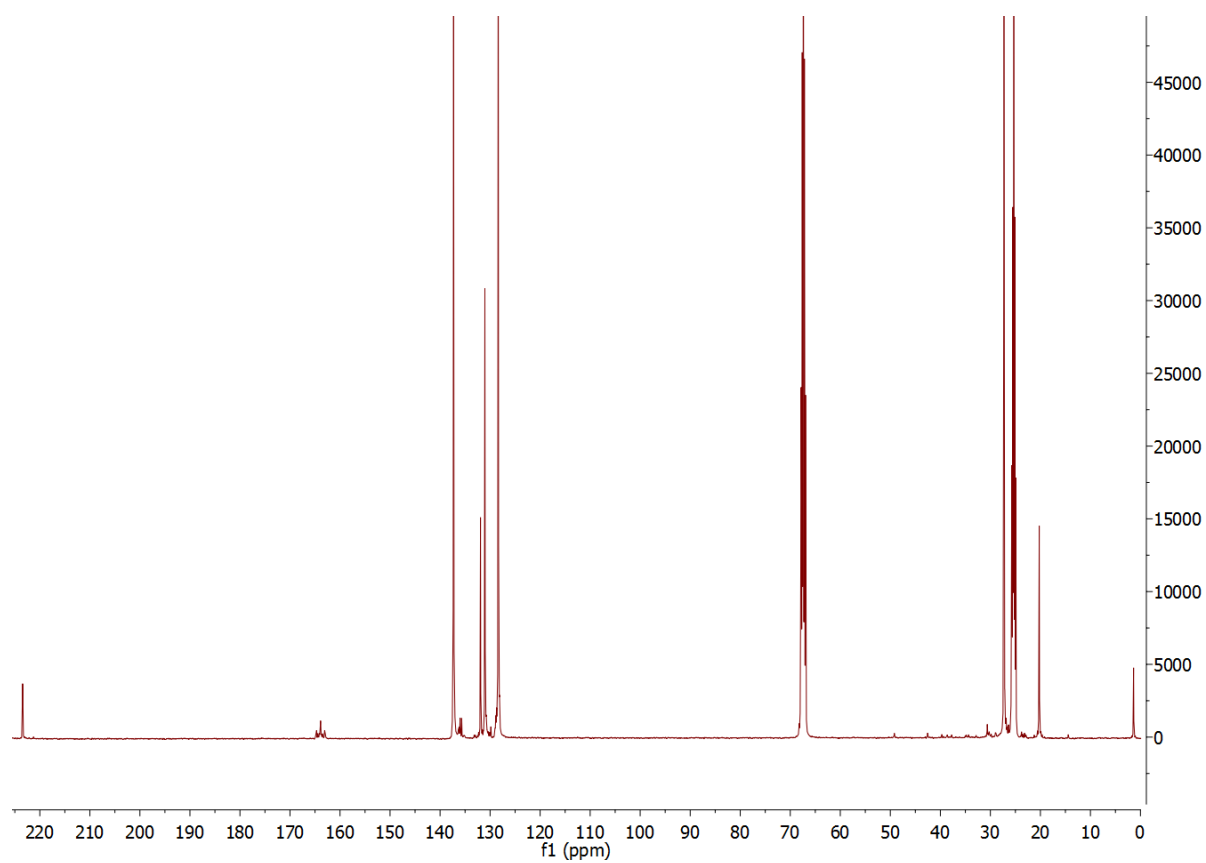


Figure S17: ^{31}P -NMR spectrum of compound **8**

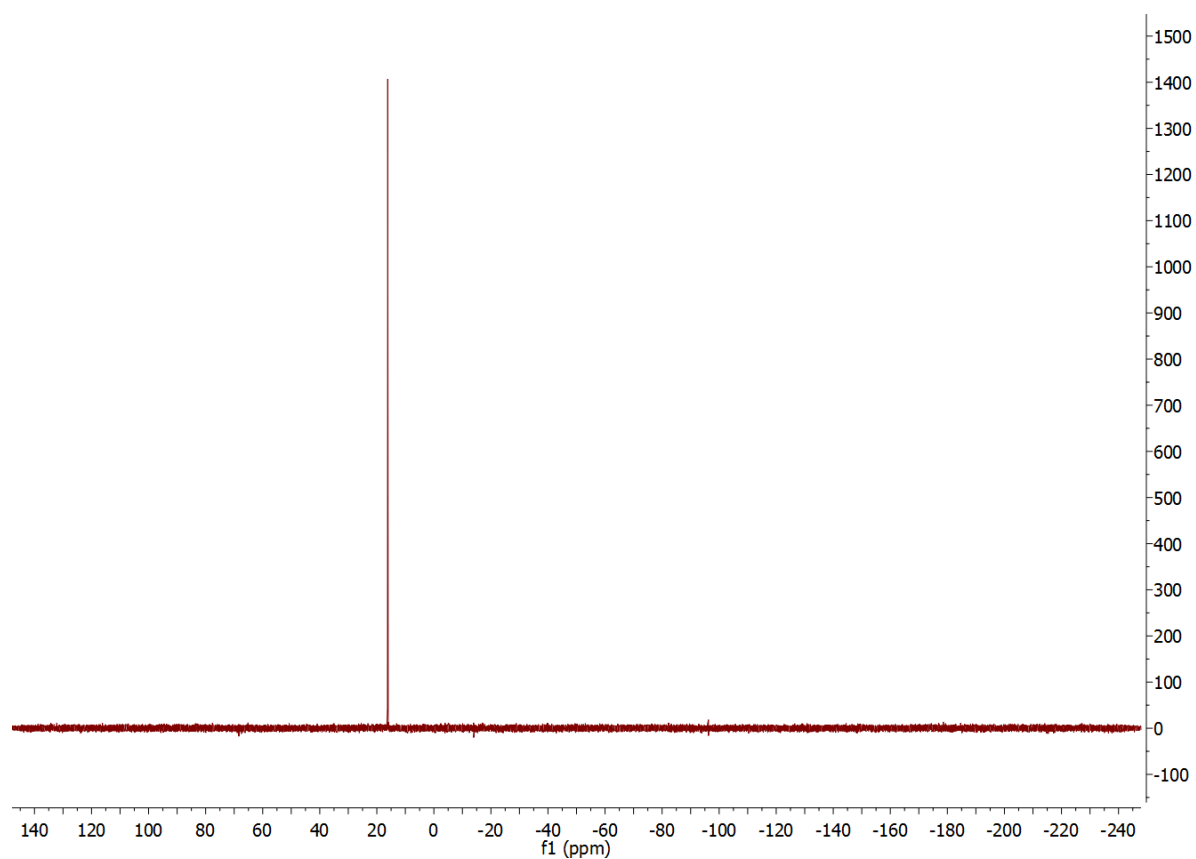


Figure S18: ^1H -NMR spectrum of compound **8**

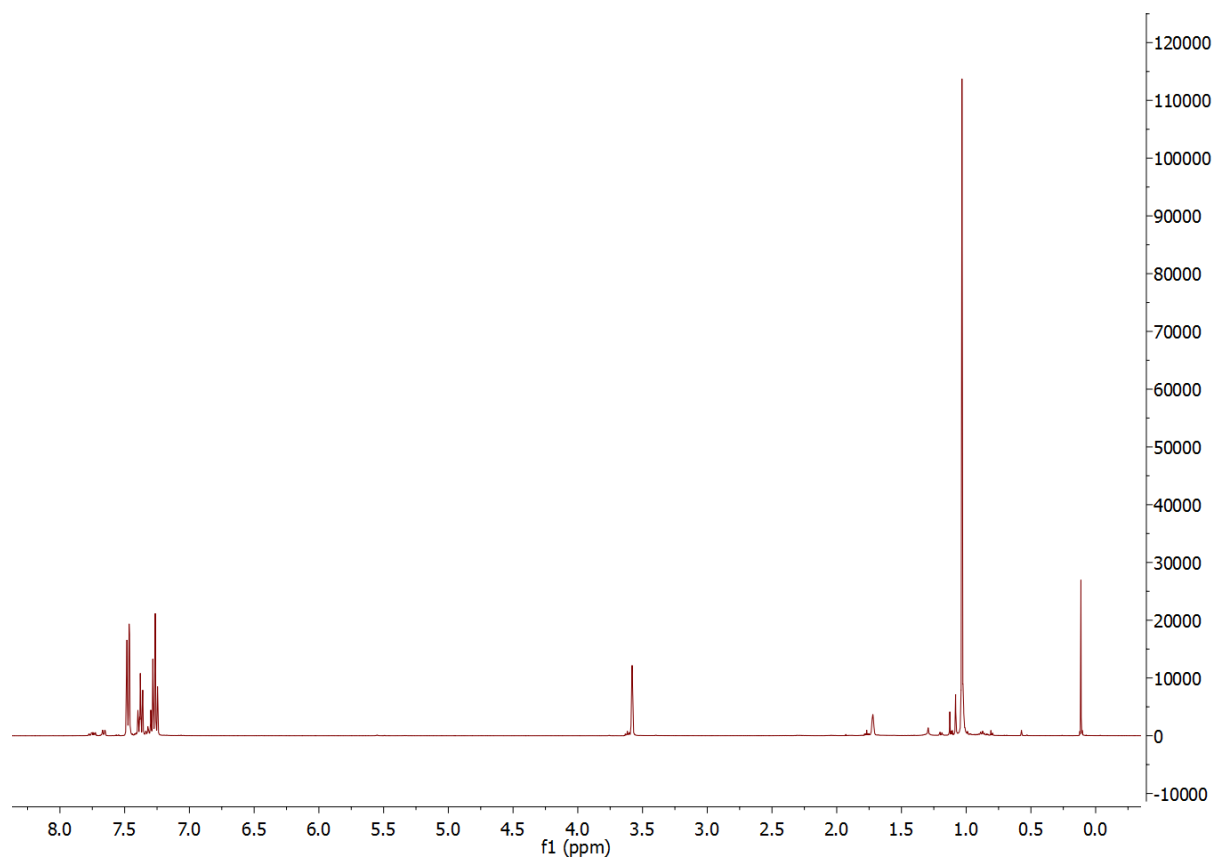
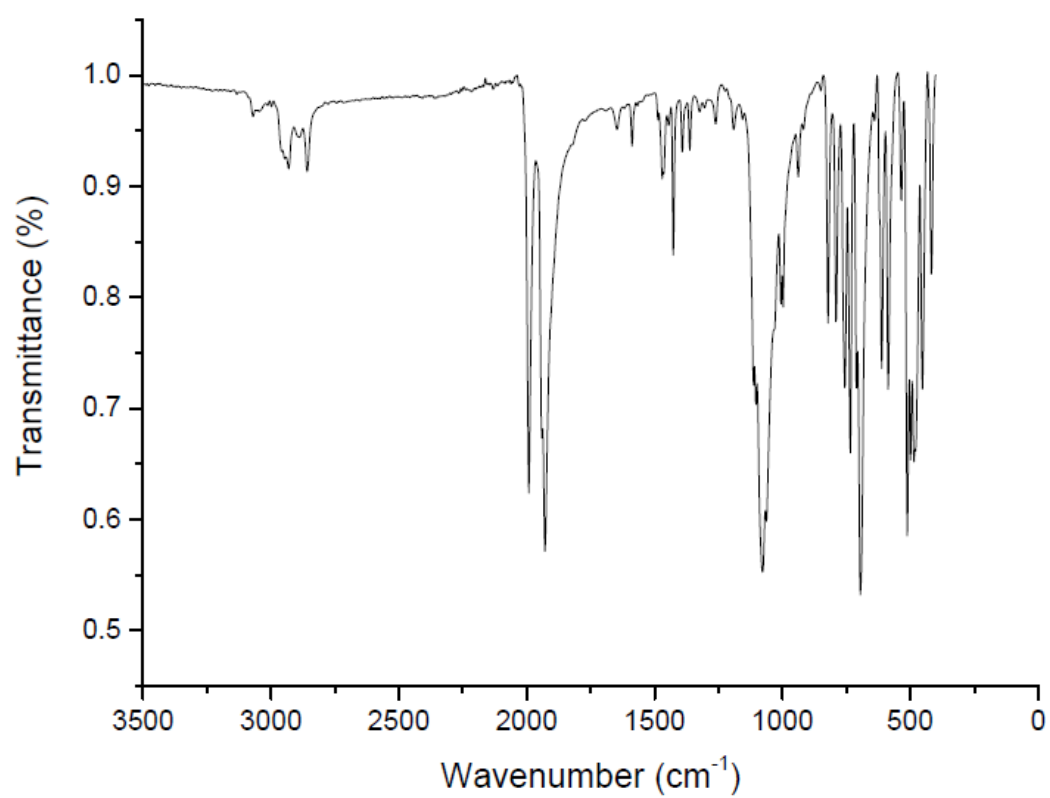


Figure S19: Solid state ATR-IR spectrum of compound **8**



X-Ray:

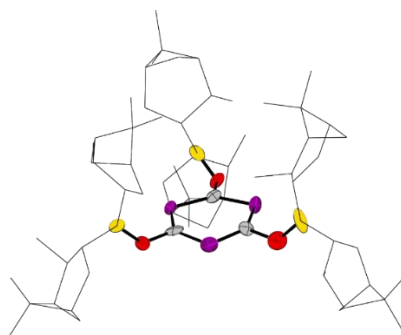


Table 2: Crystal data and structure refinement for **4**

Identification code	CCDC 1454807
Empirical formula	C ₆₃ H ₁₀₂ B ₃ O ₃ P ₃
Formula weight	1032.78
Temperature/K	102(2)
Crystal system	tetragonal
Space group	P4 ₁ 2 ₁ 2
a/Å	18.7009(7)
b/Å	18.7009(7)
c/Å	35.7978(11)
$\alpha/^\circ$	90
$\beta/^\circ$	90
$\gamma/^\circ$	90
Volume/Å ³	12519.4(10)
Z	8
$\rho_{\text{calc}}/\text{g cm}^{-3}$	1.096
μ/mm^{-1}	0.136
F(000)	4512.0
Crystal size/mm ³	0.41 × 0.38 × 0.36
Radiation	MoK α (λ = 0.71073)
2 θ range for data collection/ $^\circ$	5.948 to 52.744
Index ranges	-19 ≤ h ≤ 14, -23 ≤ k ≤ 9, -41 ≤ l ≤ 44
Reflections collected	27398
Independent reflections	12802 [R_{int} = 0.0936, R_{sigma} = 0.1790]
Data/restraints/parameters	12802/173/761
Goodness-of-fit on F ²	1.135
Final R indexes [$I \geq 2\sigma(I)$]	R_1 = 0.1259, wR_2 = 0.1623
Final R indexes [all data]	R_1 = 0.2003, wR_2 = 0.1883
Largest diff. peak/hole / e Å ⁻³	0.26/-0.23
Flack parameter	-0.03(8)

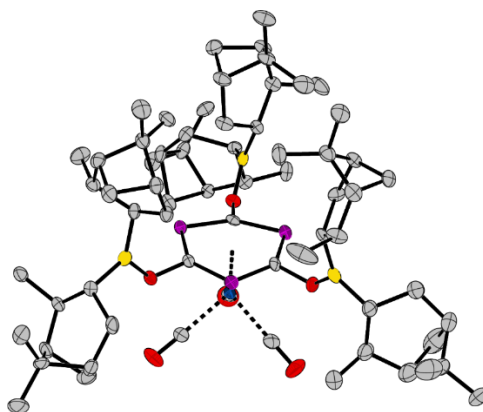


Table 3: Crystal data and structure refinement for **7**

Identification code	CCDC 1454806
Empirical formula	C ₆₆ H ₁₀₂ B ₃ MoO ₆ P ₃
Formula weight	1212.75
Temperature/K	103.2
Crystal system	orthorhombic
Space group	P2 ₁ 2 ₁ 2 ₁
a/Å	12.0176(3)
b/Å	22.3006(6)
c/Å	27.1067(8)
α/°	90
β/°	90
γ/°	90
Volume/Å ³	7264.6(3)
Z	4
ρ _{calc} /cm ³	1.109
μ/mm ⁻¹	0.290
F(000)	2592.0
Crystal size/mm ³	0.14 × 0.08 × 0.06
Radiation	MoKα (λ = 0.71073)
2θ range for data collection/°	4.53 to 52.742
Index ranges	-14 ≤ h ≤ 15, -27 ≤ k ≤ 26, -33 ≤ l ≤ 32
Reflections collected	62795
Independent reflections	14496 [R _{int} = 0.0864, R _{sigma} = 0.0887]
Data/restraints/parameters	14496/0/730
Goodness-of-fit on F ²	0.917
Final R indexes [I ≥ 2σ (I)]	R ₁ = 0.0408, wR ₂ = 0.0803
Final R indexes [all data]	R ₁ = 0.0611, wR ₂ = 0.0861
Largest diff. peak/hole / e Å ⁻³	0.31/-0.79
Flack parameter	-0.021(15)

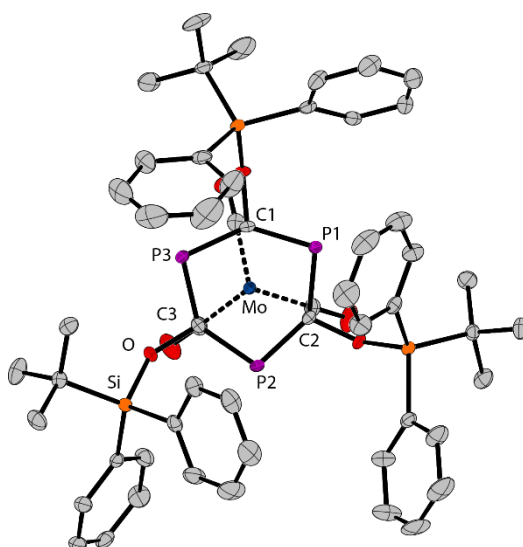


Table 4: Crystal data and structure refinement for **8**.

Identification code	CCDC 1454805
Empirical formula	$C_{27}H_{28.5}Mo_{0.5}O_3P_{1.5}Si_{1.5}$
Formula weight	537.56
Temperature/K	103.7
Crystal system	orthorhombic
Space group	Pbca
$a/\text{\AA}$	11.2701(6)
$b/\text{\AA}$	28.2269(17)
$c/\text{\AA}$	34.153(2)
$\alpha/^\circ$	90
$\beta/^\circ$	90
$\gamma/^\circ$	90
Volume/ \AA^3	10864.7(11)
Z	16
$\rho_{\text{calc}}/\text{cm}^3$	1.315
μ/mm^{-1}	0.443
$F(000)$	4464.0
Crystal size/ mm^3	$0.2 \times 0.05 \times 0.05$
Radiation	MoK α ($\lambda = 0.71073$)
2θ range for data collection/ $^\circ$	4.33 to 52.876
Index ranges	$-14 \leq h \leq 13$, $-35 \leq k \leq 35$, $-42 \leq l \leq 42$
Reflections collected	462805
Independent reflections	11168 [$R_{\text{int}} = 0.0955$, $R_{\text{sigma}} = 0.0218$]
Data/restraints/parameters	11168/0/613
Goodness-of-fit on F^2	1.085
Final R indexes [$I \geq 2\sigma(I)$]	$R_1 = 0.0309$, $wR_2 = 0.0606$
Final R indexes [all data]	$R_1 = 0.0429$, $wR_2 = 0.0649$
Largest diff. peak/hole / $e \text{\AA}^{-3}$	0.36/-0.46

Selected distances [\AA] and angles [$^\circ$] for **7 and **8**:**

[Mo{P₃C₃[OB(ipc)₂]₃}(CO)₃] (7**):**

C-O	1.142(5), 1.139(5), 1.136(5) \AA
Mo-C	2.326(4), 2.360(4), 2.339(3) \AA
Mo-P	2.5999(10), 2.6110(11), 2.5981(11) \AA

Mo-active plane of ring 1.733 \AA

[Mo{P₃C₃[OSi^{*t*}Bu(Ph)₂]₃}(CO)₃] (8**):**

C-O	1.144(2), 1.141(2), 1.143(2) \AA
Mo-C	2.3834(17), 2.3733(17), 2.3348(17) \AA
Mo-P	2.6113(5), 2.6302(5), 2.6279(5) \AA

Mo-active plane P₃C₃ ring 1.753 \AA

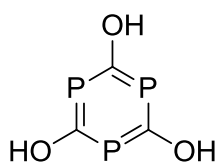
Calculations:

The electronic effect of σ -withdrawing/ π -electron donating ($R = \text{NH}_2$) and σ -donating/ π -withdrawing substituents ($R = \text{SiH}_3$) on the relative energies of the two isomers was calculated. The results are collected in Table 5. As expected, the difference in the energy between the two isomers is remarkably smaller than in the case of the silicon analogues ($R_3\text{Si-OCP}$ is higher in energy than $R_3\text{Si-PCO}$ for $R = \text{H}$ by $14.1 \text{ kcal mol}^{-1}$, for $R = \text{Ph}$ by $7.9 \text{ kcal mol}^{-1}$).^[6] For methyl and amino substituents the two isomers have practically the same energy (in range of the expected accuracy of the method), but the oxyphosphaalkyne species are thermodynamically slightly more stable. The electron withdrawing silyl group (SiH_3), however strongly favours the phosphaketene isomer by $11.6 \text{ kcal mol}^{-1}$.)

Table 5: Relative energies (in kcal mol^{-1}) of the $R_2\text{B-PCO}$ and $R_2\text{B-OCP}$ isomers at the CBS-QB3 level of theory.

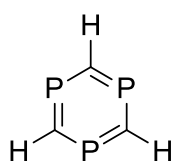
R	$R_2\text{B-PCO}$	$R_2\text{B-OCP}$
Me	1.4	0.0
NH_2	2.9	0.0
SiH_3	0.0	11.6

All following calculations were carried out using the Gaussian 09 quantum mechanical package.^[7] Geometry optimizations of the model compound were carried out using density functional theory (DFT) at the B3LYP/6-311+G** level of theory. The same level of theory has been successfully applied earlier for $(\text{PCH})_3$.^[8] At each of the optimized structures vibrational analysis was performed to ensure that the geometry corresponds to an energy minimum. For transition states first order saddle points were located with one imaginary vibration frequency, which indicates the movement of the atoms corresponding to the expected transformations along the reaction coordinates.



NPA Charge
P: +0.53
C: -0.34
O: -0.67
H: +0.48

NCIS(0): -8.2319
NCIS(1): -8.1240



NPA Charge
P: +0.77
C: -1.01
H: +0.24

NCIS(0): -4.9561
NCIS(1): -8.6446

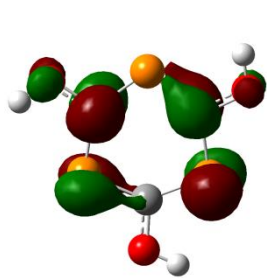


NPA Charge
C: -0.21
H: +0.21

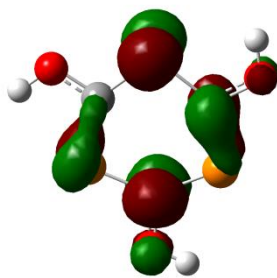
NCIS(0): -8.0388
NCIS(1): -10.2167

Scheme 1: NPA charges and NCIS^[9] values in the center and 1 Å above the plane at the B3LYP/6-311+G** level.

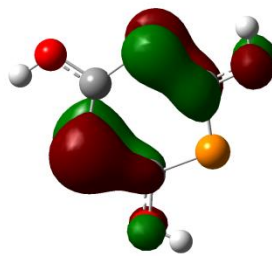
The MO of (PCOH)₃ (Isovalue = 0.05)



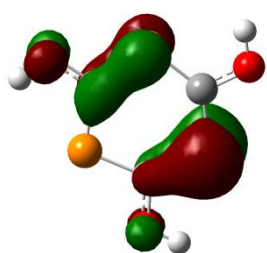
LUMO+1 (−0.08487)



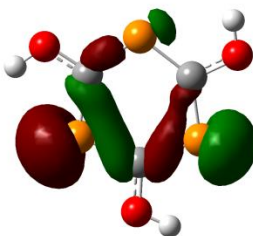
LUMO (−0.08487)



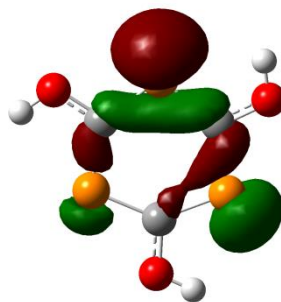
HOMO (−0.24173)



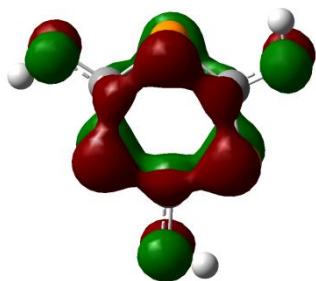
HOMO-1 (−0.24173)



HOMO-2 (−0.28510)

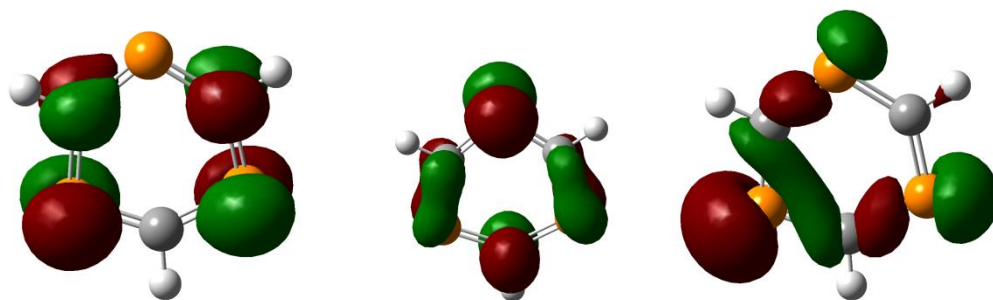


HOMO-3 (−0.28511)

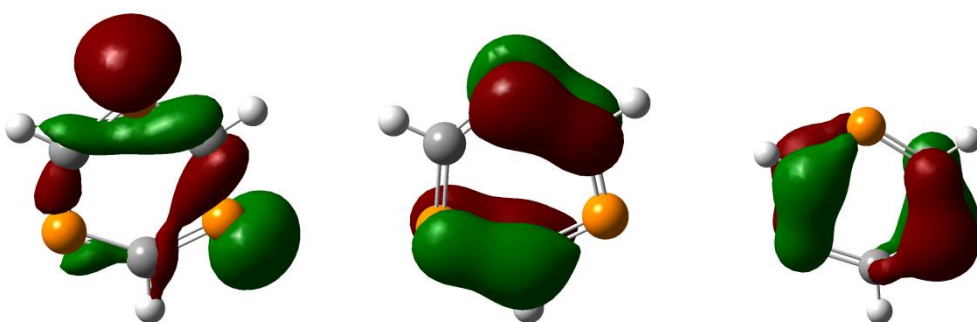


HOMO-4 (−0.29651)

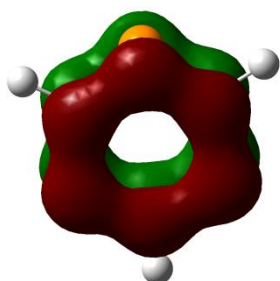
The MO of (PCH)₃ (Isovalue = 0.05)



LUMO+1 (−0.09866) LUMO (−0.09867) HOMO (−0.26872)

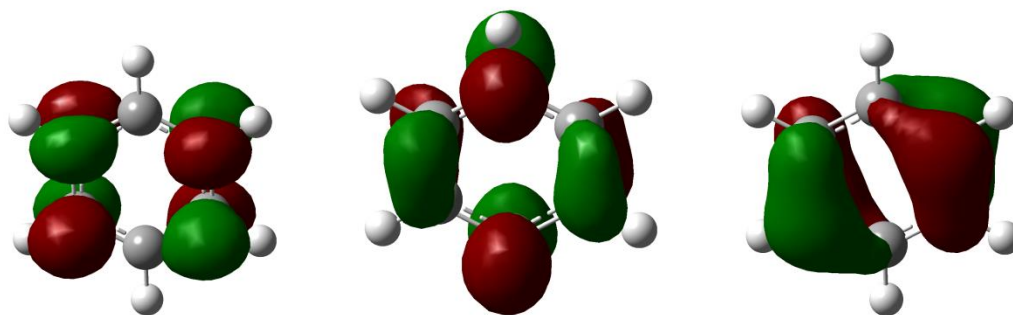


HOMO-1 (−0.26873) HOMO-2 (−0.27660) HOMO-3 (−0.27660)

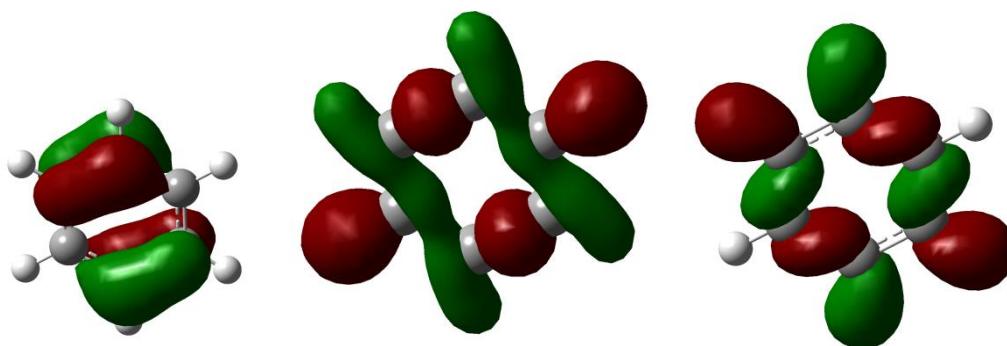


HOMO-4 (−0.35356)

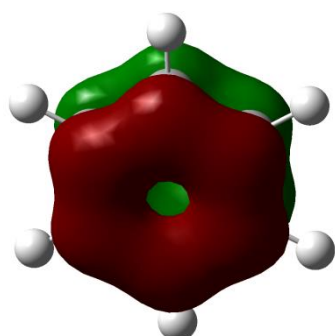
The MO of Benzene (Isovalue = 0.05) (in Hartree)



LUMO+1 (−0.01756) LUMO (−0.01756) HOMO (−0.26013)

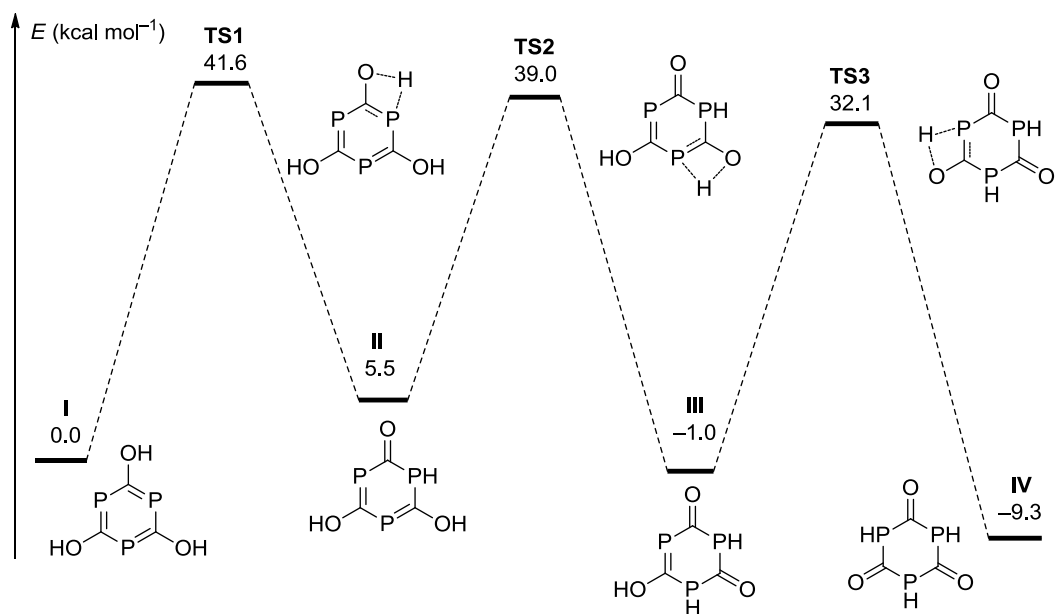


HOMO-1 (−0.26014) HOMO-2 (−0.35090) HOMO-3 (−0.35094)



24	—	□	—	0.00459	
23	—	□	—	−0.01756	□
22	—	□	—	−0.01756	□
21	—	□	—	−0.26013	□
20	—	□	—	−0.26014	□
19	—	□	—	−0.35090	□
18	—	□	—	−0.35094	□
17	—	□	—	−0.37317	■
16	—	□	—	−0.42801	

HOMO-4 (−0.37317)



Scheme 2: Relative energies of P₃C₃(OH)₃ tautomers and MERP of a possible rearrangement in the gas-phase calculated from I to IV (DFT; B3LYP/6-311+G**). Note that IV has not a planar but twisted structure. The planar isomer of IV is calculated as a saddle point with three imaginary frequency and the energy is 44.9 kcal mol⁻¹ higher than I)

XYZ Coordinate (B3LYP/6-311+G**)

PCH

E = -1140.24574960, ZPE = 0.051710

C	-1.58352800	0.19645300	-0.00010000
C	0.62161500	-1.46961600	-0.00002900
C	0.96189900	1.27313100	0.00005100
H	-2.66407000	0.33048200	-0.00004000
H	1.04578300	-2.47246900	0.00002400
H	1.61824500	2.14193800	0.00009600
P	1.83486700	-0.22762100	-0.00002300
P	-0.72029900	1.70284000	0.00000800
P	-1.11456000	-1.47520300	0.00004200

(PCOH)₃

E = -1365.9691366, ZPE = 0.064734

C	-0.55858500	-1.50556400	-0.00009500
C	-1.02454800	1.23657700	-0.00008400
C	1.58323300	0.26898100	-0.00009500
O	-1.94909600	2.24549100	-0.00006700
H	-1.51133800	3.10879700	-0.00004600
O	2.91928700	0.56511200	-0.00010700
H	3.44780700	-0.24580100	-0.00010600
O	-0.97040500	-2.81059900	-0.00009900
H	-1.93694300	-2.86243600	-0.00009800
P	0.65111500	1.76312900	0.00008000
P	-1.85243700	-0.31769800	0.00007400
P	1.20142700	-1.44546800	0.00011800

TS1

E = -1365.89714722, ZPE = 0.058962

C	-1.39929100	-0.83105300	0.03836500
C	1.43256600	-0.67622000	-0.05461100
C	0.01821300	1.60912000	0.06397500
O	2.56579000	-1.43301400	-0.07139900
H	3.35344000	-0.87222900	-0.12555200
O	-0.34558000	2.73804700	0.53544600
H	-1.67729000	2.25103500	0.41438900
O	-2.58780500	-1.46068600	0.19101300
H	-2.45560200	-2.40618700	0.36029000
P	1.70290900	1.06875100	-0.06448600
P	0.05489200	-1.81231900	0.14136600
P	-1.53038200	0.85433600	-0.48861200

Int1

E = -1365.95750578, ZPE = 0.061897

C	1.42470800	-0.73615700	-0.02839000
C	-1.36493900	-0.79441200	0.05655100
C	-0.12433800	1.73148600	-0.14947000
O	-2.40325400	-1.67165000	0.15677700
H	-3.24630400	-1.19716100	0.21875000
O	-0.08310600	2.87059200	-0.55428400
H	2.36911000	1.49831900	-0.37741900
O	2.69018300	-1.18365300	-0.21924900
H	2.69111900	-2.12249900	-0.46253800
P	-1.76759900	0.88938300	0.04447500
P	0.11373400	-1.83628400	-0.19373600
P	1.45005800	0.97980300	0.56813400

TS2

E = -1365.89810473, ZPE = 0.055924

C	0.73612500	1.38759800	0.00437000
C	-1.60727300	0.02408200	-0.02762700
C	1.02378500	-1.41452700	0.19497400
O	-2.93030200	-0.20099400	0.13902400
O	1.54982200	-2.34549800	0.74609000
O	1.51723800	2.31302400	0.41433100
P	-0.79990300	-1.58796900	-0.36553900
P	-1.04587600	1.66341400	0.04580700
P	1.85775700	0.06548600	-0.53484300
H	-3.40819600	0.62732900	0.30149900
H	2.51447600	1.39943500	0.30826500
H	-1.29584200	-2.25590700	0.78300700

Int2

E = -1365.96474405, ZPE = 0.058816

C	0.65852200	1.55241000	0.20039000
C	-1.55643000	-0.31331800	-0.02143200
C	1.13132400	-1.31505300	0.04536800
O	-2.90873800	-0.35914200	0.09845300
H	-3.20726700	-1.26403600	0.28015700

O	1.92361800	-2.17497500	0.35383900
H	2.86439000	0.43476600	0.37380900
O	1.02540800	2.48168200	0.87282300
H	-1.72473100	2.00877300	0.76316500
P	-0.67853400	-1.78774900	0.09026100
P	-1.13025800	1.43982800	-0.39181700
P	1.83177900	0.32763600	-0.58937800

TS3

E = -1365.90620926-, ZPE = 0.052905

C	1.52164600	-0.83346600	0.12361000
C	-0.03399100	1.56201500	0.03124700
C	-1.47089500	-0.85751800	0.12529100
O	0.16690000	2.65093800	0.65828900
O	-2.38253300	-1.37858100	0.70935200
O	2.44088900	-1.41527300	0.64051300
P	-1.68475300	0.96705800	-0.42861300
P	1.60772500	0.94762900	-0.40827900
P	0.01162400	-1.84958500	-0.47868700
H	1.46851400	2.30923100	0.64939700
H	-0.00178000	-2.75331000	0.61087500
H	-2.38828700	1.38467200	0.72729600

Final

E = -1365.97504138, ZPE = 0.055794

C	1.64759700	-0.36896900	0.12944100
C	-0.50427400	1.61091400	0.13008000
C	-1.14327600	-1.24211800	0.12973500
O	-0.81410900	2.60014100	0.74212100
O	-1.84511400	-2.00443000	0.74247300
O	2.65913200	-0.59539300	0.74153300
P	-1.82829800	0.40928800	-0.48744300
P	1.26885800	1.37886700	-0.48669200
P	0.55953400	-1.78827200	-0.48681800
H	1.89033900	2.05374000	0.59007000
H	0.83295800	-2.66298700	0.59080000
H	-2.72424800	0.60949700	0.58887200

Final_Plane (Three imaginary frequencies)

E = -1365.88493234, ZPE = 0.052086

C	-1.45862100	1.13955200	0.00021900
C	-0.25757700	-1.83287400	0.00002400
C	1.71622400	0.69337800	-0.00020200
O	-0.42656400	-3.03519500	0.00017400
O	2.84191200	1.14831000	-0.00022300
O	-2.41544200	1.88700400	0.00050300
P	1.40211600	-1.09536000	0.00033500
P	-1.64964100	-0.66654600	-0.00053500
P	0.24756800	1.76184000	-0.00006400
H	-2.94504000	-1.19018500	0.00013500
H	0.44194000	3.14537900	0.00002900
H	2.50305100	-1.95549100	-0.00008900

- [1] D. Heift, Z. Benkő, H. Grützmacher, *Dalton Trans.* **2014**, 43, 831-840.
- [2] C. J. Breheny, J. M. Kelly, C. Long, S. O'Keeffe, M. T. Pryce, G. Russell, M. M. Walsh, *Organometallics* **1998**, 17, 3690-3695.
- [3] R. Gleiter, H. Lange, P. Binger, J. Stannek, C. Krueger, J. Bruckmann, U. Zenneck, S. Kummer, *Eur. J. Inorg. Chem.* **1998**, 1619-1621.
- [4] P. Binger, S. Leininger, J. Stannek, B. Gabor, R. Mynott, J. Bruckmann, C. Krueger, *Angew. Chem., Int. Ed. Engl.* **1995**, 34, 2227-2230.
- [5] C. W. Tate, P. B. Hitchcock, G. A. Lawless, Z. Benkő, L. Nyulaszi, J. F. Nixon, *C. R. Chim.* **2010**, 13, 1063-1072.
- [6] D. Heift, Z. Benkő, H. Grützmacher, *Dalton Trans.* **2014**, 43, 5920-5928.
- [7] M. J. T. Frisch, G. W.; Schlegel, H. B.; Scuseria, G. E.; Robb, M. A.; Cheeseman, J. R.; Scalmani, G.; Barone, V.; Mennucci, B.; Petersson, G. A.; Nakatsuji, H.; Caricato, M.; Li, X.; Hratchian, H. P.; Izmaylov, A. F.; Bloino, J.; Zheng, G.; Sonnenberg, J. L.; Hada, M.; Ehara, M.; Toyota, K.; Fukuda, R.; Hasegawa, J.; Ishida, M.; Nakajima, T.; Honda, Y.; Kitao, O.; Nakai, H.; Vreven, T.; Montgomery, Jr., J. A.; Peralta, J. E.; Ogliaro, F.; Bearpark, M.; Heyd, J. J.; Brothers, E.; Kudin, K. N.; Staroverov, V. N.; Kobayashi, R.; Normand, J.; Raghavachari, K.; Rendell, A.; Burant, J. C.; Iyengar, S. S.; Tomasi, J.; Cossi, M.; Rega, N.; Millam, N. J.; Klene, M.; Knox, J. E.; Cross, J. B.; Bakken, V.; Adamo, C.; Jaramillo, J.; Gomperts, R.; Stratmann, R. E.; Yazyev, O.; Austin, A. J.; Cammi, R.; Pomelli, C.; Ochterski, J. W.; Martin, R. L.; Morokuma, K.; Zakrzewski, V. G.; Voth, G. A.; Salvador, P.; Dannenberg, J. J.; Dapprich, S.; Daniels, A. D.; Farkas, Ö.; Foresman, J. B.; Ortiz, J. V.; Cioslowski, J.; Fox, D. J., Gaussian 09, Revision A.1 ed., Gaussian, Inc., Wallingford CT, **2009**.
- [8] I. Păulescu, M. Medeleanu, M. Ștefănescu, F. Peter, R. Pop, *Heteratom Chem.* **2015**, 26, 206–214.
- [9] a) A. Savin, B. Silvi, F. Colonna, *Can. J. Chem.* **1996**, 74, 1088-1096; b) P. V. Schleyer, C. Maerker, A. Dransfeld, H. J. Jiao, N. J. R. V. Hommes, *J. Am. Chem. Soc.* **1996**, 118, 6317-6318)